

## Large amplitude magnetization dynamics and the suppression of edge modes in a single nanomagnet

P. S. Keatley, P. Gangmei, M. Dvornik, R. J. Hicken, J. R. Childress et al.

Citation: *Appl. Phys. Lett.* **98**, 082506 (2011); doi: 10.1063/1.3560457

View online: <http://dx.doi.org/10.1063/1.3560457>

View Table of Contents: <http://apl.aip.org/resource/1/APPLAB/v98/i8>

Published by the [American Institute of Physics](#).

---

### Related Articles

Directional-dependent coercivities and magnetization reversal mechanisms in fourfold ferromagnetic systems of varying sizes

*J. Appl. Phys.* **113**, 013901 (2013)

Magnetoresistance and shot noise in graphene-based nanostructure with effective exchange field

*J. Appl. Phys.* **112**, 123719 (2012)

Thermally assisted spin-transfer torque magnetization reversal in uniaxial nanomagnets

*Appl. Phys. Lett.* **101**, 262401 (2012)

Combined fitting of alternative and direct susceptibility curves of assembled nanostructures

*J. Appl. Phys.* **112**, 123902 (2012)

Thermal fluctuations of magnetic nanoparticles: Fifty years after Brown

*App. Phys. Rev.* **2012**, 13 (2012)

---

### Additional information on *Appl. Phys. Lett.*

Journal Homepage: <http://apl.aip.org/>

Journal Information: [http://apl.aip.org/about/about\\_the\\_journal](http://apl.aip.org/about/about_the_journal)

Top downloads: [http://apl.aip.org/features/most\\_downloaded](http://apl.aip.org/features/most_downloaded)

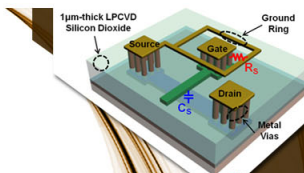
Information for Authors: <http://apl.aip.org/authors>

## ADVERTISEMENT



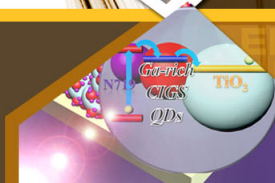
**EXPLORE WHAT'S  
NEW IN APL**

**SUBMIT YOUR PAPER NOW!**



### **SURFACES AND INTERFACES**

Focusing on physical, chemical, biological, structural, optical, magnetic and electrical properties of surfaces and interfaces, and more...



### **ENERGY CONVERSION AND STORAGE**

Focusing on all aspects of static and dynamic energy conversion, energy storage, photovoltaics, solar fuels, batteries, capacitors, thermoelectrics, and more...

# Large amplitude magnetization dynamics and the suppression of edge modes in a single nanomagnet

P. S. Keatley,<sup>1,a)</sup> P. Gangmei,<sup>1</sup> M. Dvornik,<sup>1</sup> R. J. Hicken,<sup>1</sup> J. R. Childress,<sup>2</sup> and J. A. Katine<sup>2</sup>

<sup>1</sup>*School of Physics, University of Exeter, Stocker Road, Exeter EX4 4QL, United Kingdom*

<sup>2</sup>*Hitachi Global Storage Technologies, San Jose Research Center, 3403 Yerba Buena Road, San Jose, California 95135, USA*

(Received 10 November 2010; accepted 7 February 2011; published online 25 February 2011)

Large amplitude magnetization dynamics of a single square nanomagnet have been studied by time-resolved Kerr microscopy. Experimental spectra revealed that only a single mode was excited for all bias field values. Micromagnetic simulations demonstrate that at larger pulsed field amplitudes the center mode dominates the dynamic response while the edge mode is almost completely suppressed. Controlled suppression of edge modes in a single nanomagnet has potential applications in the operation of nanoscale spin transfer torque oscillators and bistable switching devices for which the amplitude of the magnetization trajectory is often large and a more uniform dynamic response is desirable. © 2011 American Institute of Physics. [doi:10.1063/1.3560457]

Large amplitude precessional magnetization dynamics of nanoscale ferromagnetic elements are expected to facilitate increased switching speeds in bistable magnetic storage elements and the operation of spin transfer torque oscillators. Most dynamical studies have been performed on arrays of nanomagnets<sup>1,2</sup> where interelement dipolar interactions can lead to collective excitations<sup>3–6</sup> while structural variations lead to inhomogeneous broadening.<sup>2,5</sup> These phenomena can be avoided by measuring a single nanomagnet.<sup>7</sup> Recently, cavity enhancement of the magneto-optical Kerr effect was used to study magnetization dynamics in single out-of-plane magnetized Ni(150 nm) disks with diameter ranging from 5  $\mu\text{m}$  to 125 nm.<sup>8</sup> In Ref. 8 it was shown that the intrinsic properties of a single nanomagnet can no longer be observed when an ensemble of disks is measured.

The small amplitude dynamics of a square nanomagnet magnetized in-plane and along an edge is complicated by excitation of center- and edge-type modes.<sup>1,5,9</sup> The two modes coexist for a range of bias fields while maximum amplitude shifts from center to edge mode as the bias field is decreased.<sup>5</sup> Large amplitude excitation can significantly modify the spatial character.<sup>10</sup> In this work time-resolved (TR) measurements and micromagnetic simulations reveal that the large amplitude dynamics of a single nanomagnet can be dominated by the quasiuniform center mode, while the nonuniform edge mode is almost completely suppressed.

TR measurements were performed on a single 440  $\times$  440 nm<sup>2</sup> CoFe(1 nm)/NiFe(5 nm)/CoFe(1 nm) nanomagnet. The dynamics were observed experimentally by TR scanning Kerr microscopy (TRSKM) with a  $\sim$ 300 nm full-width at half maximum spot and enhanced mechanical stability. The 440 nm square was fabricated on top of the center conductor of a microscale coplanar waveguide (CPW) used to generate an in-plane pulsed magnetic field from a 7 V current pulse of <40 ps rise time and 70 ps duration. The CPW track was tapered to 4  $\mu\text{m}$  width at the sample to enhance the pulsed field amplitude and induce large amplitude dynamics. The pulsed field amplitude  $h_p$  was estimated

to be  $\sim$ 90 Oe from the Karlquist equation.<sup>11</sup> TR measurements were performed for a range of bias fields  $H_B$  applied in-plane and along either the edge of the element perpendicular to  $h_p$ , or along the element diagonal.

TR measurements (not shown) were also performed upon a 2  $\mu\text{m}$  disk of the same composition for bias fields in the range  $\pm$ 1 kOe applied parallel to the CPW and uniaxial anisotropy easy axis. A macrospin model was used to fit the precession frequency as a function of the bias field yielding values of the saturation magnetization  $M_s$  (789 emu/cm<sup>3</sup>),  $g$ -factor (2.05), and uniaxial anisotropy constant  $K_u$  (4340 ergs/cm<sup>3</sup>) that were used in micromagnetic simulations.

The simulations were performed using the object oriented micromagnetic framework (OOMMF).<sup>12</sup> A 440 nm square with rounded corners of radius 55 nm was modeled as a single layer using a mesh of cell size  $4 \times 4 \times 7$  nm<sup>3</sup> and an exchange parameter of  $13 \times 10^{-7}$  ergs/cm. Simulations with smaller cell sizes did not show any significant differences. The dynamics were excited by a pulsed field of 70 ps duration, 30 ps rise time, and amplitude ranging from 5 to 100 Oe. Micromagnetic simulations of the 2  $\mu\text{m}$  disk were in excellent agreement with the experimental data and macrospin fitting which confirmed the suitability of the material parameters for the simulations.

Figure 1 shows typical TR polar Kerr signals acquired from the square for  $H_B$  ranging from 500 to 100 Oe. In the parallel geometry [Fig. 1(a)], where  $H_B$  was applied along the edge of the square, only weak beating of some of the TR signals was observed, indicating that either the center or edge mode dominates the dynamic response. In the diagonal geometry [Fig. 1(b)], where  $H_B$  was applied along the diagonal the TR signals were found to exhibit enhanced damping and have smaller amplitude due to the smaller initial torque acting on the static magnetization.

Normalized fast Fourier transform (FFT) spectra of the TR signals are shown in Fig. 2. The experimental spectra (dark gray shading) are overlaid with spectra calculated from simulations (solid black line). A schematic of the simulated ground state is inset.<sup>13</sup> To understand the small amplitude

<sup>a)</sup>Electronic mail: p.s.keatley@exeter.ac.uk.

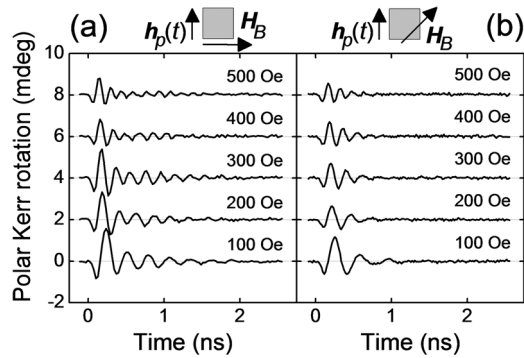


FIG. 1. TR signals acquired from the 440 nm square at different bias field values with the field applied along (a) the edge and (b) the diagonal.

response of the square, the values of the damping parameter  $\alpha$  and pulsed field amplitude  $h_p$  were initially set to 0.01 and 30 Oe, respectively, while  $M_s$  and  $K_u$  were assumed to be uniform throughout the element.

In the parallel geometry [Fig. 2(a)] the experimental spectra show a single main peak at all field values. For  $H_B$  of 300 Oe and below, the simulated spectra are in very good agreement with the experimental spectra, albeit with a much narrower linewidth. Fourier images<sup>14</sup> calculated from the simulated dynamic magnetization<sup>5</sup> confirm that the lower and higher frequency modes are of edge- and center-type respectively and coexist with equal amplitude at a “crossover field” of 400 Oe. For  $H_B$  values from 400 to 700 Oe a discrepancy of  $\sim 1$  GHz is seen between the frequencies of the center mode and the main experimental peak suggesting that the material parameters used in the simulations are not optimized.

In the diagonal geometry [Fig. 2(b)] the experimental spectra reveal a single broad peak that is consistent with the enhanced damping seen in Fig. 1(b). The frequency of the experimental peak was found to be consistently lower than that observed in the parallel geometry, and consistent with the different static internal fields in the simulations for the two geometries. Previous studies of dynamics in square elements of similar aspect ratio have also shown marked differences in dynamic behavior for the edge and diagonal cases.<sup>15,16</sup> Simulated spectra and Fourier images reveal at least two modes at all field values that are not resolved experimentally and correspond to a lower frequency center-type mode with large amplitude across the element diagonal

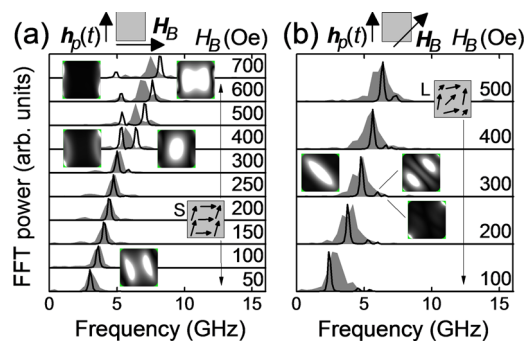


FIG. 2. (Color online) Experimental (gray shading) and simulated (black line) spectra for the (a) parallel and (b) diagonal geometries. Simulated spectra assume uniform  $M_s$ ,  $\alpha=0.01$ , and  $h_p=30$  Oe. The spatial character of the modes is shown in images of FFT magnitude (inset). For all  $H_B$  the square was in the S- and leaf-state (L) in (a) and (b) respectively.

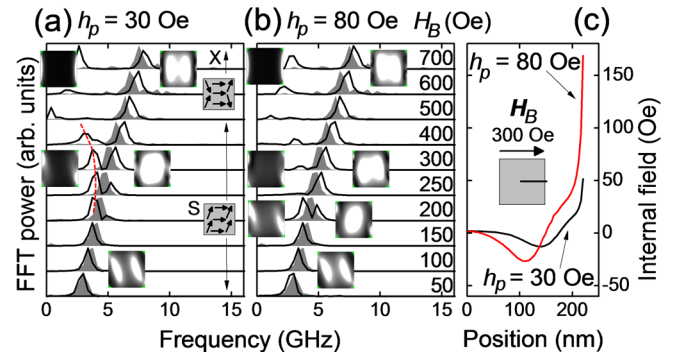


FIG. 3. (Color online) Experimental (gray shading) and simulated (black line) spectra for the parallel geometry. Simulated spectra assume reduced edge  $M_s$ ,  $\alpha=0.03$ , and  $h_p$  of 30 Oe (a) and 80 Oe (b). The spatial character of typical modes is shown in images of FFT magnitude (inset). The ground state is shown inset in (a) and changes from X to S as  $H_B$  is reduced below 600 Oe. Cross sections (see inset) of the difference in the internal field  $H_i$  between successive precession antinodes of opposite polarity are shown in (c) for  $h_p=30$  and 80 Oe.

orthogonal to  $H_B$ , and two higher frequency low amplitude modes localized near to the corners along  $H_B$ .

In comparing experiment and simulation for the parallel geometry, the good agreement of the lower frequency edge mode and poor agreement of the higher frequency center mode is surprising. The edge mode frequency is more easily shifted and split by shape variations or edge roughness,<sup>2,5</sup> while the center mode frequency is dominated by the magnetic parameters of the material. Nanofabrication processes can lead to a reduction in  $M_s$  at the edges of a nanomagnet<sup>17</sup> that affects the evolution of its spin-wave modes.<sup>18</sup> Simulations assuming values  $M_s$  and  $K_u$  reduced  $\times 0.8$  resulted in a shift in the whole spectra so that the agreement at 300 Oe and below was less good.

An improvement in the overall agreement between experiment and simulation for all values of  $H_B$  was achieved by reducing  $M_s$  at the edge of the square by 20% using a two-dimensional profile of form  $\cos^6(2\pi x/l)\cos^6(2\pi y/l)$ , where  $l=440$  nm and  $x, y$  are the spatial coordinates. The value of  $\alpha$  was adjusted so that the simulations reproduced the relaxation observed in the experiment, yielding values of 0.03 and 0.05 for the parallel and diagonal cases, respectively. Furthermore, the value of  $h_p$  was varied from 5 to 100 Oe in the simulations to understand its effect.<sup>19</sup>

Figure 3 shows experimental spectra acquired in the parallel geometry overlaid with simulated spectra for the square with reduced edge  $M_s$  and  $\alpha=0.03$ . In Figs. 3(a) and 3(b) the value of  $h_p$  was 30 Oe and 80 Oe, respectively. In Fig. 3(a) the simulated center mode and the experimental spectra are in better agreement between 700 and 200 Oe (now within  $\sim 500$  MHz), while the edge mode is still in good agreement below 200 Oe. Further quantitative improvement might be achieved by tuning the profile of  $M_s$ . The crossover field has shifted from 400 to 300 Oe while the experimental linewidth is reproduced by the larger value of  $\alpha$ . However, at 200 Oe the simulated frequency of the edge mode begins to shift from that of the experimental spectra as  $H_B$  increases (dashed line). In Fig. 3(b) simulated spectra for  $h_p=80$  Oe reveal a remarkable suppression of the edge mode amplitude between 400 and 250 Oe and improved agreement with the experimental spectra. Furthermore, the crossover field has now shifted to 200 Oe indicating that for larger values of  $h_p$  the



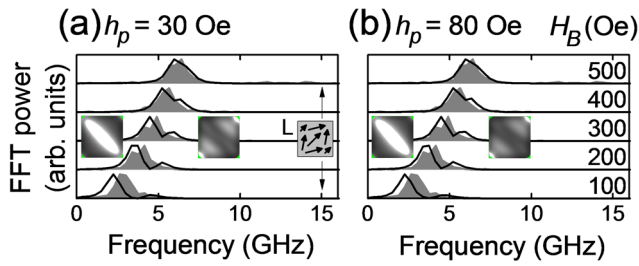


FIG. 4. (Color online) Experimental (gray shading) and simulated (black line) spectra are shown for the diagonal geometry. Simulated spectra assume reduced edge  $M_s$ ,  $\alpha=0.05$ , and  $h_p$  of 30 Oe (a) and 80 Oe (b). The character of the modes is shown in images of FFT magnitude (inset) for the leaf state (L).

excitation of the center mode is favored at lower  $H_B$  values. The onset of edge mode suppression can be observed in the simulated spectra for a  $h_p$  value as small as 10 Oe.<sup>19</sup>

Since the laser spot size is smaller than the square highly localized edge modes in the simulations at large  $H_B$  (e.g., 2.75 GHz at 700 Oe) are probed by the Gaussian tail of the optical probe. Therefore, sensitivity to edge modes for  $H_B > 500$  Oe is diminished so that they were not observed experimentally. The simulations also reveal instability of the ground state following the onset of the pulsed field resulting in variations in both the frequency and amplitude of the edge mode for  $H_B > 500$  Oe as the value of  $h_p$  was increased.<sup>19</sup> For  $H_B$  smaller than 500 Oe but greater than the crossover field the edge mode extends more toward the central region of the element where it is more readily detected. However, weaker coupling of the edge mode to the large amplitude field<sup>10</sup> and modification of the internal magnetic field  $H_i$  lead to the suppression of the edge mode. Cross sections of the component of  $H_i$  parallel to  $H_B$  were extracted from the simulations at  $H_B=300$  Oe for precession antinodes of opposite polarity. The difference in  $H_i$  is shown in Fig. 3(c) for  $h_p=30$  and 80 Oe. For  $h_p=80$  Oe the large amplitude excitation of the center mode leads to a greater modification to  $H_i$  in the region of the edge mode than for  $h_p=30$  Oe. Therefore, the nonuniform profile of  $H_i$  that gives rise to edge mode localization is continuously modified due to precession associated with the center mode and no longer supports the edge mode.

Figure 4 shows the experimental spectra acquired in the diagonal geometry overlaid with simulated spectra for the square with reduced edge  $M_s$  and  $\alpha=0.05$ . In Figs. 4(a) and 4(b) the value of  $h_p$  was 30 Oe and 80 Oe, respectively. Remarkably, the pulsed field amplitude has a negligible effect upon the spectra since  $H_i$  is more resistant to modification in the leaf state.<sup>13</sup> Fourier images reveal that the higher frequency mode is highly localized and may not be observed experimentally.

A possible explanation for the observed differences in the linewidth and the deduced values of  $\alpha$  in the parallel and diagonal geometries may involve magnon–magnon scattering, which is not included in the micromagnetic model. In this work, only modes that couple strongly to a uniform pulsed field are excited and detected. However, square nanomagnets can support a large number of asymmetric modes of similar frequency<sup>5</sup> that offer many channels for dissipation

via magnon–magnon scattering. The efficiency of such scattering depends upon the ground state, the internal field, and the frequencies of the modes,<sup>20</sup> and therefore leads to differences in the relaxation for the parallel and diagonal geometries.

In summary TRSKM measurements of large amplitude magnetization dynamics within a single nanomagnet have been performed with excellent signal-to-noise ratio. Quantitative agreement between experimental and simulated spectra was found to depend upon the profile of  $M_s$  throughout the element while variations in the damping imply that the micromagnetic model does not fully describe the relaxation of the dynamics. Such effects would be difficult to isolate in closely packed arrays. As device volumes decrease a larger amplitude excitation is required to generate a detectable signal. This work shows that a large amplitude excitation can modify the character of the resonant mode spectra in addition to the magnetic ground state and yield a more uniform dynamic response.

The authors gratefully acknowledge financial support from the EU Grant MASTER No. NMP-FP7-212257 and the UK Engineering and Physical Sciences Research Council.

- <sup>1</sup>V. V. Kruglyak, A. Barman, R. J. Hicken, J. R. Childress, and J. A. Katine, *Phys. Rev. B* **71**, 220409(R) (2005).
- <sup>2</sup>J. M. Shaw, T. J. Silva, M. L. Schneider, and R. D. McMichael, *Phys. Rev. B* **79**, 184404 (2009).
- <sup>3</sup>V. V. Kruglyak, P. S. Keatley, A. Neudert, R. J. Hicken, J. R. Childress, and J. A. Katine, *Phys. Rev. Lett.* **104**, 027201 (2010).
- <sup>4</sup>S. Tacchi, M. Madami, G. Gubbiotti, G. Carlotti, H. Tanigawa, T. Ono, and M. P. Kostylev, *Phys. Rev. B* **82**, 024401 (2010).
- <sup>5</sup>P. S. Keatley, V. V. Kruglyak, A. Neudert, E. A. Galaktionov, R. J. Hicken, J. R. Childress, and J. A. Katine, *Phys. Rev. B* **78**, 214412 (2008).
- <sup>6</sup>V. V. Kruglyak, S. O. Demokritov, and D. Grundler, *J. Phys. D: Appl. Phys.* **43**, 264001 (2010).
- <sup>7</sup>Z. Liu, R. D. Sydora, and M. R. Freeman, *Phys. Rev. B* **77**, 174410 (2008).
- <sup>8</sup>A. Barman, S. Wang, J. D. Maas, A. R. Hawkins, S. Kwon, A. Liddle, J. Bokor, and H. Schmidt, *Nano Lett.* **6**, 2939 (2006).
- <sup>9</sup>G. Gubbiotti, M. Madami, S. Tacchi, G. Carlotti, A. O. Adeyeye, S. Goolaup, N. Singh, and A. N. Slavin, *J. Magn. Magn. Mater.* **316**, e338 (2007).
- <sup>10</sup>V. E. Demidov, M. Buchmeier, K. Rott, P. Krzysteczko, J. Münchenberger, G. Reiss, and S. O. Demokritov, *Phys. Rev. Lett.* **104**, 217203 (2010).
- <sup>11</sup>J. P. Nibarger, R. Lopusnik, Z. Celinski, and T. J. Silva, *Appl. Phys. Lett.* **83**, 93 (2003).
- <sup>12</sup>M. Donahue and D. G. Porter, OOMMF User's Guide, Version 1.0, NISTIR 6376 (National Institute of Standards and Technology, Gaithersburg, MD, 1999), see <http://math.nist.gov/oommf>.
- <sup>13</sup>O. Fruchart and A. Thiaville, *C. R. Phys.* **6**, 921 (2005).
- <sup>14</sup>The calculated Fourier images show the spatial character of FFT magnitude where white is large amplitude and black is zero.
- <sup>15</sup>A. Barman, V. V. Kruglyak, R. J. Hicken, A. Kundrotaitė, and M. Rahman, *Appl. Phys. Lett.* **82**, 3065 (2003).
- <sup>16</sup>V. V. Kruglyak, P. S. Keatley, R. J. Hicken, J. R. Childress, and J. A. Katine, *Phys. Rev. B* **75**, 024407 (2007).
- <sup>17</sup>S. Cornelissen, L. Bianchini, A. Helmer, T. Devolder, J.-V. Kim, M. O. de Beeck, W. Van Roy, L. Lagae, and C. Chappert, *J. Appl. Phys.* **105**, 07B903 (2009).
- <sup>18</sup>Z. Zeng, K. H. Cheung, H. W. Jiang, I. N. Krivorotov, J. A. Katine, V. Tiberkevich, and A. Slavin, *Phys. Rev. B* **82**, 100410 (2010).
- <sup>19</sup>See supplementary material at <http://dx.doi.org/10.1063/1.3560457> for simulated spectra for a range of values of the pulsed field amplitude.
- <sup>20</sup>H. Schultheiss, C. W. Sandweg, B. Obry, S. Hermsdorfer, S. Schafer, B. Leven, and B. Hillebrands, *J. Phys. D: Appl. Phys.* **41**, 164017 (2008).